


## Fluorescence quantum yield of CDOM in coastal zones of the Arctic seas

Anastasia N. Drozdova, Marina D. Kravchishina, Daria A. Khundzhua, Mihail P. Freidkin & Svetlana V. Patsaeva


To cite this article: Anastasia N. Drozdova, Marina D. Kravchishina, Daria A. Khundzhua, Mihail P. Freidkin & Svetlana V. Patsaeva (2018): Fluorescence quantum yield of CDOM in coastal zones of the Arctic seas, International Journal of Remote Sensing, DOI: [10.1080/01431161.2018.1506187](https://doi.org/10.1080/01431161.2018.1506187)

To link to this article: <https://doi.org/10.1080/01431161.2018.1506187>

 View supplementary material 

 Published online: 22 Aug 2018.

 Submit your article to this journal 

 Article views: 32

 View Crossmark data 



# Fluorescence quantum yield of CDOM in coastal zones of the Arctic seas

Anastasia N. Drozdova <sup>a</sup>, Marina D. Kravchishina<sup>a</sup>, Daria A. Khundzhua<sup>b</sup>,  
Mihail P. Freidkin<sup>b</sup> and Svetlana V. Patsaeva<sup>b</sup>

<sup>a</sup>Shirshov Institute of Oceanology, Russian Academy of Sciences, Moscow, Russia; <sup>b</sup>Faculty of Physics, Lomonosov Moscow State University, Moscow, Russia

## ABSTRACT

Along with traditional optical indices, calculated from absorption and fluorescence spectra to describe chromophoric dissolved organic matter (CDOM) naturally occurring in water, the fluorescence quantum yield (FQY) becomes significant. Knowledge of CDOM optical properties is important for satellite remote sensing as well as for lidar ground-true measurements. The FQY as a function of excitation wavelength within 240–500 nm range for a variety of the Arctic shelf waters was determined for the first time in order to identify the characteristic chromophores peculiar to different regions of the Arctic basin affected by freshwater runoff. The surface water samples were collected during several cruises in 2015–2017 in the following sites: the mouth areas of the Khatanga and Lena Rivers (the Laptev Sea), the delta area of the Northern Dvina River (the White Sea), desalinated waters of the Kara Sea (influenced by freshwater of the Ob and Yenisei Rivers) and the East Siberian Sea (influenced by freshwaters of the Indigirka and Kolyma Rivers), as well the shelf areas of those seas not affected by terrigenous runoff. To characterize DOM, conventional optical indices SR, HIX, and BIX were calculated. In most cases, important humic character of DOM was established, while the contribution of autochthonous organic matter varied from low to intermediate level. For the samples with terrestrial impact, the FQY decreased from excitation at 240 nm to 270–280 nm and then increased, demonstrating two peaks at 340 and 380 nm, with constant decrease towards longer excitation wavelengths; at  $\lambda_{\text{ex}} = 380$  nm FQY varied from 1.4% to 3.1%. In some cases, additional maximum at 270 nm of FQY-excitation dependency was observed as an indicator of autochthonous nature of biological material. Minimal FQY was measured for the White Sea surface waters, the maximal for the Laptev and East Siberian seas.

## ARTICLE HISTORY

Received 5 February 2018  
Accepted 18 July 2018

## 1. Introduction

The Arctic Ocean and Arctic shelf seas are important components of the global climate system, and at the same time represent the most sensitive regions to climate change.

**CONTACT** Anastasia N. Drozdova [adrozдова@ocean.ru](mailto:adrozдова@ocean.ru) Shirshov Institute of Oceanology, Russian Academy of Sciences, Moscow, Russia

Supplemental data for this article can be accessed [here](#).

© 2018 Informa UK Limited, trading as Taylor & Francis Group

Physical processes, taking place there, influence regional and global oceanic circulation, heat and mass transfer through water exchange with the Atlantic and Pacific Oceans (Kostianoy and Nihoul 2009). Recently the growing interest in the Arctic region is noted. This is due to climate changes observed in the Arctic in the last decades and their strong effect on Arctic shelf (David et al. 2009; Meier et al. 2014). Dissolved organic matter (DOM) of natural origin is one of the key elements of the Arctic aqueous ecosystem (Vetrov and Romankevich 2004). Large continental rivers play an important role in regional carbon cycling by transporting terrigenous material from land to the ocean (Mann et al. 2016), including roughly  $3 \times 10^{13}$  g of dissolved organic carbon (DOC) (Amon 2004; Raymond et al. 2007).

The study of DOM in natural water is carried out by a variety of methods. The DOC content is determined by high-temperature combustion; the origin and degree of organic matter degradation are examined analysing biomarkers (for example, the distribution of n-alkanes and lignin phenols), with the gas- and liquid- chromatography. The mass-spectrometry, optical techniques, including analysis of absorption and fluorescence spectra, are widely used to characterize DOM (Thurman 2012). DOM fractions are successfully analysed using chromatographic techniques (Trubetskoi and Trubetskaya 2004; Trubetskoj, Trubetskaya, and Richard 2009; Trubetskaya, Richard, and Trubetskoj 2015) and their combination with online detection of absorption and fluorescence (Parlanti, Morin, and Vacher 2002; Trubetskaya, Richard, and Trubetskoj 2015; Khundzhua et al. 2017; Wunsch, Murphy, and Stedmon 2017). The very informative approach is the ultrahigh resolution Fourier transform ion cyclotron mass spectrometry (Marshall, Hendrickson, and Jackson 1998; Hockaday et al. 2009), that allows distinguishing the signals of individual molecular ions of humic substances (HS), the main component of organic matter (OM) of terrestrial origin. However, this technique, as well as investigation of biomarkers usually require large sample volume, sample pre-treatment, for example, pre-concentration and extraction, and therefore cannot be carried out on a routine base in the ship laboratories due to the fine-tuning of specialized instruments used.

In contrary, optical techniques, such as satellite imagery (Kutser et al. 2009; Mannino et al. 2014), lidar remote sensing (Fantoni et al. 2004; Chekalyuk and Hafez 2013; Palmer et al. 2013; Pelevin et al. 2017), onboard laboratory (Lubben et al. 2009) and *in situ* measurements (Harsdorf et al. 1999; Grunwald et al. 2007), do not require any sample preparation. Such methods are perfectly suited for field studies, providing a much higher temporal and spatial resolution compared with conventional chemical techniques (Orek et al. 2013; Palmer et al. 2013). A lot of widely used methods for investigation of DOM distribution and dynamics are based on measurement of the fluorescence response of its chromophoric fraction (CDOM). A typical spectrum of UV-excited CDOM fluorescence in natural waters involves two superimposed bands. The first one represents a peak at 300–350 nm and is attributed to the emission of proteins, aromatic amino acids, and phenolic compounds, while the second band with a maximum at 380–480 nm is due to fluorescence of HS (Stedmon and Nelson 2015; Coble 2007). The most advanced approach for studying CDOM fluorescence is the decomposition of excitation-emission matrix spectra by parallel factor analysis (Stedmon, Markager, and Bro 2003; Wunsch, Murphy, and Stedmon 2017). It is targeted to distinguish individual fluorophores associated with different CDOM components but requires significant training data set,

laborious measurements of fluorescence over wide ranges of excitation and emission wavelengths, and non-trivial data processing. Simpler approaches, for instance, evaluation of biological autochthonous (BIX) and humification (HIX) indices (Huguet et al. 2009), slopes of the absorption spectra within different wavelength ranges ( $S_{UVA}$ ,  $S_{UVB}$ ,  $S$ ) and their ratio,  $S_R$  (Leenheer and Croue 2003), cannot give a complete description of CDOM. Therefore, the search for new optical proxies is undoubtedly of interest for oceanographic studies. One of the prospective but yet poorly studied characteristics of CDOM optical properties is the fluorescence quantum yield (FQY).

FQY for dye molecules represents the probability of a fluorophore to emit light while returning to its ground state after being excited by light of higher frequency, and defined as the ratio of the number of photons emitted to the number of photons absorbed (Lakowicz 2006). For CDOM representing a pool of organic compounds with vast structural and compositional diversity, the FQY is therefore referred as the apparent fluorescence quantum yield (Wünsch, Murphy, and Stedmon 2015). Thus, both types of spectra are needed to determine FQY and to examine the relationship between fluorescent and absorption properties of CDOM.

The FQY of natural waters has been an object of several studies. FQY at discrete excitation wavelength in the UV was measured for various freshwater and marine samples (see, for example, Zepp and Schlotzhauer 1981; Hawes, Carder, and Harvey 1992; Shubina et al. 2010; Ferrari 2000) and fractions of various molecular size for riverine CDOM (Gorshkova et al. 2005; Milyukov et al. 2007). Colloidal OM had lower FQY values compared to low-molecular DOM fractions. Fluorescence quantum yield was found essentially dependent on excitation wavelength increasing its value with the excitation wavelength rising from 270 to 355 nm. Contrasting to aquatic CDOM, the FQY for commercial humic acids and preparations made of carbon material was lower and practically had no dependence on excitation wavelength up to 355 nm of excitation (Shubina et al. 2010; Gosteva et al. 2012). FQY at an excitation wavelength of 355 nm was found to be higher in the cold upper Mediterranean waters (upwelling), as well as in the deep waters of the Atlantic at the summit of the seamounts: 1.18% and 1.06%, respectively. For comparison, the averaged values found are 0.91 and 0.96 in the surface waters in the Rhine and Rhone river plumes, respectively. The values were slightly higher at the euphotic depth: 0.99% and 1.00% (Ferrari 2000). Fewer studies were focused on wavelength dependence of FQY of natural CDOM in attempt to better characterize its variations and linkage to CDOM composition. In the study of Green and Blough (1994) a wavelength dependence of FQY of CDOM from marine, riverine, and estuarine waters from south Florida waters, the Amazon River, the Tamiami River, and Suwannee River fulvic acid was evaluated for the first time. Other areas of investigation of CDOM FQY from coastal margins receiving terrestrial input included natural waters across the Equatorial Atlantic Ocean (Andrew et al. 2013), deep and surface waters of Norwegian Sea (Wünsch, Murphy, and Stedmon 2015), waters of the Satilla River (USA) (Zepp, Sheldon, and Moran 2004). Investigation of Suwannee River fulvic and humic acids was published in (Del Vecchio and Blough 2004). In all the cases FQY of CDOM as a function of wavelength exhibited two maxima at 340–355 and 370–400 nm with moderate variations discussed in details in Section 4.2.

Our previous measurements performed in the coastal zones of the Kara Sea in 2015 showed that FQY upon excitation at 370 nm varies from 0.6% to 3% for CDOM in surface

waters (Drozdoва, Patsaeva, and Khundzhua 2017). FQY for each CDOM sample was described as a function of excitation wavelength within 250–550 nm. The FQY demonstrated non-monotonic dependence: its value was decreasing from excitation wavelength of 250 nm to 270–280 nm, and then it was rising demonstrating two peaks located at 340 and 380 nm with constant further decrease towards longer excitation wavelengths. We, therefore, resume that FQY and its dependences on excitation wavelengths in the wide range of their alteration may represent a perspective optical characteristics for CDOM studies, especially in the Arctic coastal waters, since each river system is characterized by its unique DOM composition (Lobbjes, Fitznar, and Kattner 2000). Such studies of FQY for CDOM in the Arctic region were practically not carried out, with the exception of our above-mentioned one and the work of Wunsch, Murphy, and Stedmon (2017). In this paper, we continue studying CDOM optical properties for the surface waters in the coastal zone of the Arctic Ocean. Data from multiple cruises were combined to carry out a comparison of FQY between water areas influenced by different rivers. Thus, the spatial variability of CDOM FQY was measured in the White Sea and Siberian Shelf waters in the Kara, Laptev and East Siberian seas. In total, 28 seawater samples were investigated, for 12 of which the FQY was measured in the range from 250 to 500 nm, and for the rest 14 samples at three excitation wavelengths of 270, 310 and 355 nm. To judge the DOM composition, we evaluated optical indices, such as the biological index, the humification index, and spectral slopes. To identify the influence of mixing, salinity was used as the indicator of freshwater contribution. A modest number of the studied samples does not allow to draw conclusions on FQY as a potential proxy for biogeochemical processes and DOM dynamics. However, the typical values of FQY and its variability, depending on the degree of desalination of the surface layer and the mutual contribution of the autochthonous and allochthonous components of DOM, are of interest to a broad scientific community studying the DOM biogeochemistry in the Arctic Ocean with use of absorption and fluorescence spectroscopy.

## 2. Field sampling and methods

### 2.1. Sampling areas

The water samples were collected in summer-autumn season during the 65<sup>th</sup> (Kara and Laptev seas, 2015), 68<sup>th</sup> (Northern Dvina River delta area, White Sea, 2017) and 69<sup>th</sup> (Laptev and East Siberian seas, 2017) cruises of the RV *Akademik Mstislav Keldysh*. Three stations were chosen to study the FQY of CDOM in the Kara Sea, see [Figure 1](#). Low impact of riverine waters was exhibited near the Novaya Zemlya Trough (station 5199, salinity 31.7). The station 5205, located on a transect across desalinated surface waters along the eastern coast of Novaya Zemlya, was characterized by minimal salinity of 16.4 (Drozdoва, Patsaeva, and Khundzhua 2017). The last station, 5214, showing a pronounced influence of Ob and Yenisei rivers runoff (Makkaveev et al. 2017), was sited near the St. Anna Trough. Five samples were taken on a transect along the 130° meridian in the Laptev Sea, see [Figure 1](#). Salinity varied between 3.0 in the Lena Delta region and 30.1 near the continental slope. The presence of more saline waters compared to closely located stations 5220 and 5223, was recorded at the station 5215–2 (Sukhanova et al. 2017; Stepanova, Polukhin, and Kostyleva 2017). It was demonstrated that the

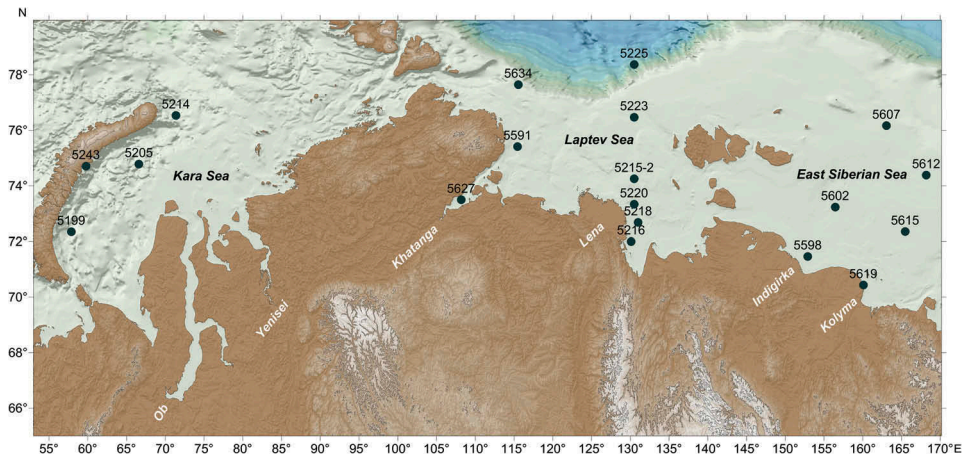


**Figure 1.** The map showing location of hydrological stations in the 65<sup>th</sup> and 69<sup>th</sup> cruises of the RV *Akademik Mstislav Keldysh*.

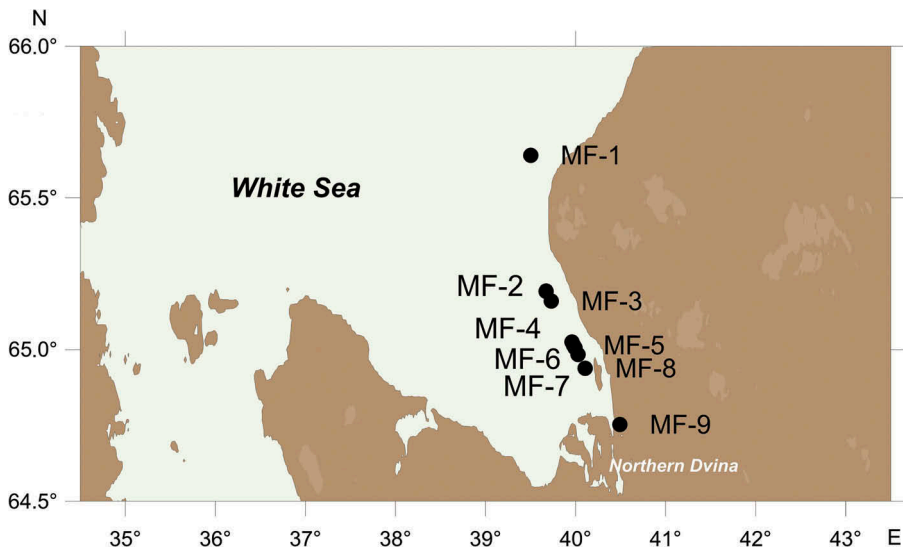


**Figure 2.** The map showing location of hydrological stations in the 68<sup>th</sup> cruise of the RV *Akademik Mstislav Keldysh*.

pycnocline at the station 5215-2 locally elevated to the surface, dividing the desalinated region into two parts due to orographic upwelling. Ten water samples were collected during the 69<sup>th</sup> cruise of the RV *Akademik Mstislav Keldysh* in September 2017 from the surface waters of the Laptev and East Siberian seas, see Figure 1. The hydrological stations were located along three transects from the estuarine regions of the Khatanga, Indigirka and Kolyma rivers to the continental slope across salinity gradients 3.5–30.1, 15.1–30.0, and 17.0–29.3, respectively (Drozdova, Krylov, and Shchuka 2018).

Analysis of the origin and distribution of CDOM within the Laptev and East Siberian seas have shown that desalinated waters of the Laptev Sea were formed due to the

Khatanga River runoff and had important humic character up to water salinity 22.3. In the East Siberian Sea, the conditions were completely different. Within that area, autochthonous substances emitting protein-like fluorescence under excitation at 270–280 nm represent an essential component of CDOM along with weak humic character. The Delta region of the Northern Dvina River (the White Sea) was studied in more detail. Location of 9 hydrological stations, MF-1–MF-9, with surface water salinity varying from 0 to 24.5 are shown in [Figure 2](#).

## **2.2. Sampling**

Seawater samples from the Kara, Laptev and East Siberian seas were collected using Niskin bottles of 5 L volume mounted on a rosette device with CTD and filtered using precombusted ( $t = 450^{\circ}\text{C}$ ) Whatman GF/F filters of 0.7  $\mu\text{m}$  nominal pore size. All samples were stored in dark glass vials at  $t = 4^{\circ}\text{C}$  until further analysis. Water samples from the area of the Northern Dvina River mouth were collected from the surface layer using a bucket in the course of the vessel. Water salinity was analyzed onboard immediately after sampling.

## **2.3. Spectral measurements and fluorescence quantum yield calculation**

Absorption spectra in the range from 200 to 900 nm were detected using Solar PB2201 spectrophotometer in quartz cuvettes with an optical path length of 1, 3 or 5 cm. Absorbances, measured with 3 or 5 cm cells, were normalized to 1 cm optical path. Fluorescence emission spectra were recorded with the Solar CM2203 luminescence spectrometer in standard quartz cuvettes for fluorimetry with excitation wavelengths altering in the range from 240 to 550 nm, while special attention was paid to recording emission spectra with excitation at 270, 310 and 355 nm (see some examples of absorption and emission spectra in Supplementary material, Fig. S1, S2). This choice of certain excitation wavelengths is associated with our previous studies, which showed the most important features in CDOM fluorescence spectra (Patsayeva and Reuter 1995; Milyukov et al. 2007). Under excitation at 270 nm, one can see so-called protein-like fluorescence (Coble 2007; Trubetskaya, Richard, and Trubetskoj 2016). We note that protein-like fluorescence in natural waters with maximum around 300–350 nm could be caused not only by proteinous material, but could result from aromatic amino-acids and phenols (Patsayeva and Reuter 1995). To quantify roughly contributions of protein-like and humic-type fluorescence we calculated fluorescence intensities excited at 270 nm separately in two spectral regions, 295–370 and 370–700 nm. The excitation at 310 nm corresponds to the wavelength which provides the deepest ‘blue shift’ of CDOM fluorescence emission with alteration of excitation wavelength within the UV range (Belin et al. 1993; Shubina et al. 2010). The wavelength 355 nm is often used in lidar systems for remote sensing (Fantoni et al. 2004; Pelevin et al. 2017), so it is promising to use this wavelength to have comparable results with onboard lidar measurements in the sea.

Because at some wavelengths absorbances relative to 1 cm path exceeded 0.1, to avoid inner filter effect the correction of fluorescence spectra was performed using absorbances at the excitation wavelength and within the wavelength range of

registration. For this purpose, the detected fluorescence intensity at each emission wavelength was multiplied by  $10^{0.5(D_{\text{ex}}+D_{\text{em}})}$ , where  $D_{\text{ex}}$  and  $D_{\text{em}}$  represent absorbances at the wavelength of excitation and emission, respectively, related to optical path of 1 cm. We modified the formulae from (Wünsch et al. 2016) taking into account that the path length of excitation and emission beams inside the cell, or distance to the center of the cell, are equal to 0.5 cm.

Calculation of the FQY was carried out by the method of reference compound used earlier in our works for CDOM samples of natural water (Milyukov et al. 2007; Shubina et al. 2010; Drozdova, Patsaeva, and Khundzhua 2017) and commercial humic preparations (Gosteva et al. 2012; Yakimenko et al. 2018). The well-established photoluminescence quantum yield standard, an aqueous solution of quinine sulfate dehydrate, was used as the reference compound, since its fluorescence quantum yield is known, and emission band resembles the humic-like fluorescence of CDOM in regards to its spectral shape and the position of a maximum. The quinine sulfate dehydrate solution has the absolute fluorescence quantum yield 0.546 in aqueous 0.5 M solution of  $\text{H}_2\text{SO}_4$  (Velapoldi and Mielenz 1981). The accuracy of FQY estimation is discussed in detail in the Section 3 of Supplementary material.

To separate roughly contributions of protein-like and humic-like fluorescence bands excited at 270 nm we summarized fluorescence intensities in two spectral regions, below and above 370 nm. Overall fluorescence measured at  $\lambda_{\text{ex}} = 270$  nm was divided into two components, corresponding to intensities integrated over 280–370 nm and 370–700 nm. Since it is not possible to separate contributions of different fluorophores into absorption spectra, we calculated FQY under excitation at 270 nm as two additive parts using the same absorbance at 270 nm, namely  $\Phi(\text{UV})$  and  $\Phi(\text{humic})$ , which in total give  $\Phi(\lambda_{\text{ex}} = 270 \text{ nm})$ .

## 2.4. Optical indices

Napierian absorption coefficients  $a_\lambda$  were calculated as  $a_\lambda = A(\lambda) \times 2.303/l$ , where  $l$  equals to 0.01, 0.03, or 0.05 m (the cuvette path length in meters). Absorption spectra between 300 and 650 nm were characterized by the exponential spectral slope coefficient  $S$  defined as follows:  $a_\lambda = a_{\lambda_0} e^{-S(\lambda-\lambda_0)}$  according to (Stedmon, Markager, and Kaas 2000; Stedmon and Nelson 2015). The spectral slopes for the 275–295 nm and 350–400 nm ranges,  $S_{\text{UVB}}$  and  $S_{\text{UVA}}$ , as well as their ratio,  $S_{\text{R}}$ , were calculated using linear regression of the log-transformed functions of absorption coefficients  $a_\lambda$ .  $S_{\text{R}}$  correlates with molecular weight and the degree of photochemical degradation of CDOM, so  $S_{\text{R}} < 1$  is typical for terrestrial CDOM,  $S_{\text{R}} > 1.5$  indicates the presence of oceanic and photodegraded terrestrial CDOM (Helms et al. 2008). A specific UV absorbance (SUVA) was determined for a few samples. SUVA was calculated by normalizing the decadic absorption at 254 nm to the DOC concentration. It is used for estimating the dissolved aromatic carbon content in aquatic systems (Weishaar et al. 2003). DOC concentration for the Laptev Sea surface waters was measured by high-temperature combustion with a Shimadzu TOC- $V_{\text{CPH/CPN}}$  analyzer. In case of the samples from the White Sea, DOC values were inquired from a personal communication with Kochenkova A.I., who investigated also a distribution of suspended matter along the transect (Kochenkova, Novigatskiy, and Gordeev 2018).



Humification (HIX) and biological/autochthonous (BIX) indices were calculated to reveal the degree of maturation and autochthonous biological activity in water according to the following equations:  $HIX = \Sigma I_{em435-480} / \Sigma I_{em300-345}$  at  $\lambda_{ex} = 254$  nm (Zsolnay et al. 1999) and  $BIX = I_{em380} / I_{em430}$  at  $\lambda_{ex} = 310$  nm. DOM characteristics associated with the range of values obtained for HIX and BIX are summarized in (Huguet et al. 2009). Thus,  $HIX > 16$  and  $0.6 < BIX < 0.7$  is typical for terrigenous DOM,  $4 < HIX < 10$  and  $0.7 < BIX < 1.0$  characterizes DOM of mutual terrigenous and marine (autochthonous) origin,  $HIX < 4$  and  $BIX > 1.0$  indicates the biological or aquatic bacterial origin of DOM.

### 3. Results

#### 3.1. Northern Dvina River delta (White Sea)

Salinity, optical indices calculated from absorption spectra, and FQY determined from fluorescence spectra for the samples MF-1–MF-9 are given in Table 1. Absorption coefficient at  $\lambda = 350$  nm varied from 7.13 to 68.7  $m^{-1}$  and demonstrated a strong correlation with salinity. It is described by the following equation:  $a = 67.838 - 2.528 \times \text{Salinity}$ , and characterized by the coefficient of determination  $R^2 = 0.999$ , see Figure 3.  $S_{UVB}$ ,  $S_{UVA}$ , and  $S_R$  change slightly from fresh to marine environment.  $S_R$  amounted to 0.78–0.88 which is typical for terrestrial DOM.

The fluorescence quantum yield of CDOM for the sample MF-9 was described as a function of excitation wavelength. The FQY in Figure 4 demonstrates a non-monotonic dependence: its value first is decreasing from excitation wavelength of 250 nm to 270–280 nm, and then it is rising showing a shoulder around 340 nm and the peak values at 370–390 nm with further constant decrease towards longer excitation wavelengths. The maximal FQY of CDOM for the Northern Dvina River freshwater was found as 1.43% at 400 nm. For the rest samples, FQY was measured at discrete  $\lambda_{ex}$  equals to

**Table 1.** FQY and optical indices of CDOM for the samples collected in the White and Laptev seas.

Sample	Salinity	FQY (%)			$a_{350}$ ( $m^{-1}$ )	$S_{UVA}$ ( $\mu m^{-1}$ )	$S_{UVB}$ ( $\mu m^{-1}$ )	$S_R$	SUVA ( $m^2 g C^{-1}$ )
		270 nm	310 nm	355 nm					
White Sea (2018)									
MF-1	24.5	1.20	1.32	1.65	7.1	17.7	15.0	0.85	3.07
MF-2	18.6	1.05	1.14	1.57	20.3	16.5	14.1	0.86	3.74
MF-3	21.1	1.08	1.21	1.65	14.1	16.8	14.8	0.88	3.59
MF-4	16.0	0.97	1.07	1.58	27.5	16.3	13.6	0.83	3.84
MF-5	10.5	0.94	0.98	1.45	40.7	16.2	13.2	0.82	4.31
MF-6	6.7	0.84	0.93	1.42	49.7	16.4	13.2	0.81	4.24
MF-7	3.8	0.81	0.87	1.31	58.1	16.2	12.9	0.80	4.37
MF-8	1.3	0.76	0.82	1.24	65.2	16.5	12.9	0.78	4.34
MF-9	0.0	0.73	0.77	1.13	68.7	16.6	13.0	0.78	4.53
Transect from the Lena Delta to the continental slope (2015)									
5216	3.0	1.35	1.81	2.39	7.3	17.7	16.5	0.93	2.41
5220	17.8	1.63	1.89	2.50	5.0	18.3	17.8	0.97	2.52
5215–2	22.2	1.82	2.18	2.90	4.1	18.2	18.0	0.99	2.44
5223	20.6	1.56	1.97	2.46	5.5	18.4	17.3	0.94	2.50
5225	30.1	0.64	0.70	0.67	5.9	17.7	18.9	1.07	n/a
Transect from the Khatanga River estuary to the continental slope (2017)									
5627	3.5	0.94	1.22	1.74	12.3	16.0	16.0	1.00	n/a
5591	22.3	1.14	1.35	1.69	4.4	17.4	17.0	0.99	n/a
5634	30.1	1.78	1.01	0.81	2.1	n/a	n/a	n/a	n/a

n/a – data are not available

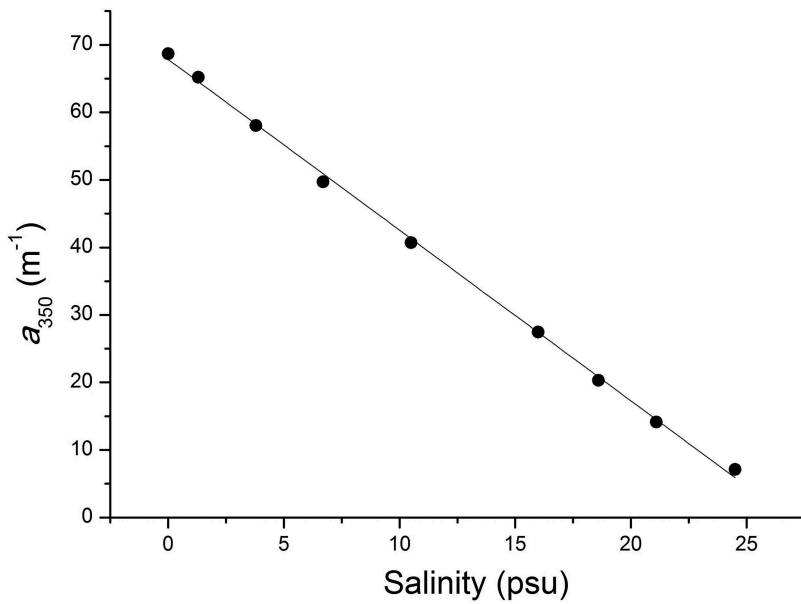


**Figure 3.** Relationship between salinity and absorption coefficient  $a_{350}$  for the White Sea water with salinity gradient along the Northern Dvina River plume.

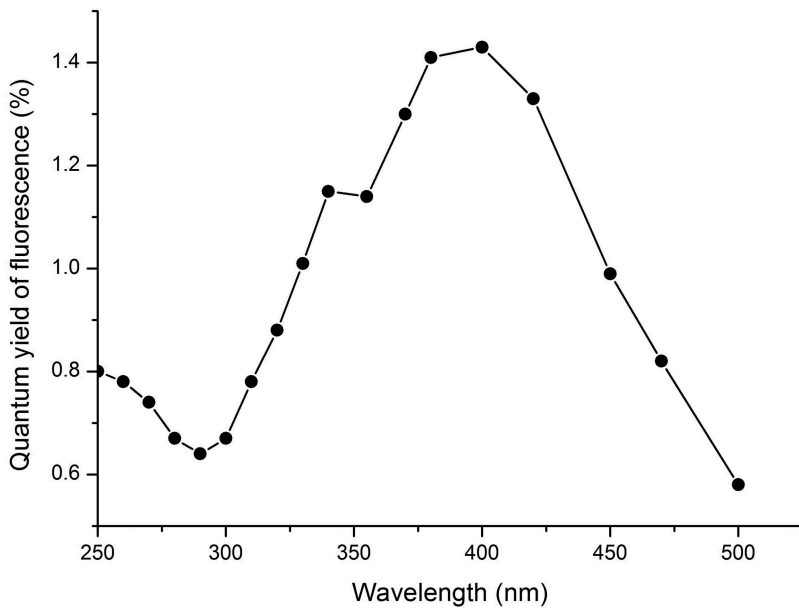


**Figure 4.** Fluorescence quantum yield of CDOM as a function of excitation wavelength for the sample MF-9 collected in the Northern Dvina River delta region.

270, 310, and 355 nm. An apparent decrease of FQY at each excitation wavelength with the decrease of salinity was observed, see Figure 5. Positive correlations are described by linear functions, characterized by the coefficients of determination equals to 0.974, 0.983 and 0.923 for excitation at 270, 310 and 355 nm, respectively. The relation

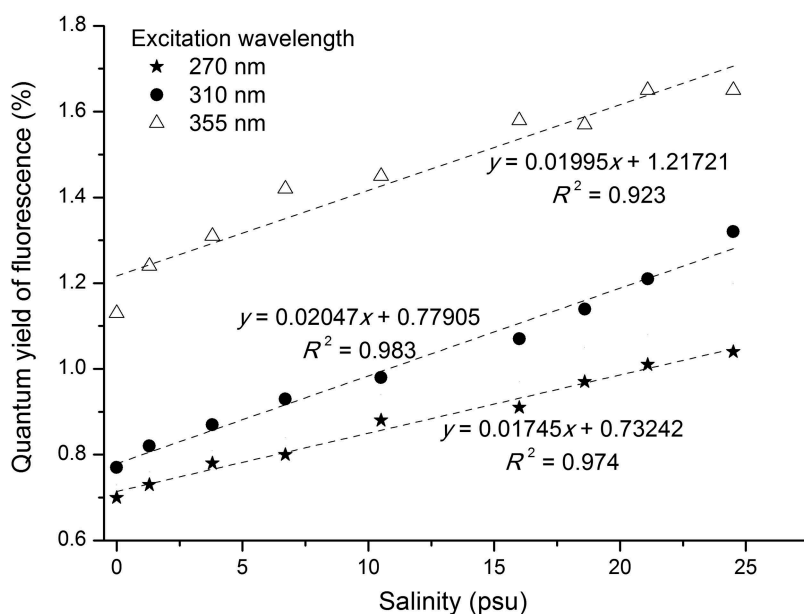


**Figure 5.** FQY of CDOM measured at excitation wavelengths 270 nm, 310 nm, and 355 nm versus water salinity for the samples MF-1–MF-9 for the White Sea water with salinity gradient along the Northern Dvina River plume.

$\Phi_{270} < \Phi_{310} < \Phi_{355}$  is valid for all the studied samples, which is in agreement with data of Shubina et al. (2010). The component of CDOM giving protein-like fluorescence and corresponding to the labile autochthonous compounds reached its maximum value of 0.16% at the station MF-1 with salinity 24.5, see Fig. S3 of Supplementary material.

### 3.2. Laptev Sea

Salinity, optical indices calculated from absorption spectra and FQY of CDOM for the samples collected in the Laptev Sea in 2015 and 2017 along two transects are given in Table 1. Absorption coefficient at  $\lambda = 350$  nm varied in a wide range from  $2.32 \text{ m}^{-1}$  in the continental slope region (station 5225) to  $12.3 \text{ m}^{-1}$  in the Khatanga River estuary.  $S_R$  values do not exceed 1.1 for all the samples indicating terrigenous origin of CDOM. Quantum yield of CDOM fluorescence was described as a function of excitation wavelength for all the seawater samples collected along the  $130^\circ\text{E}$  (Lena Delta – continental slope) as well as for the sample from the Khatanga River estuary (station 5627). FQY at excitation wavelengths 270 nm, 310 nm, and 355 nm are given in Table 1. When excited at 270 nm FQY has similar values for surface waters affected by the Lena and Khatanga rivers, while FQY at  $\lambda_{\text{ex}}$  310 or 355 nm is generally smaller for the waters influenced by terrigenous DOM supplied by the Khatanga River. Three of five seawater samples collected in September 2015 (5216, 5220, 5223) showed similar values of FQY, as well as the similar dependences on excitation wavelength, see Figure 6. The CDOM at the station 5215–2 has higher values of FQY, while at the station 5225 CDOM FQY has 5 times lower values than the ones of all other samples. Upon excitation at 355 nm FQY

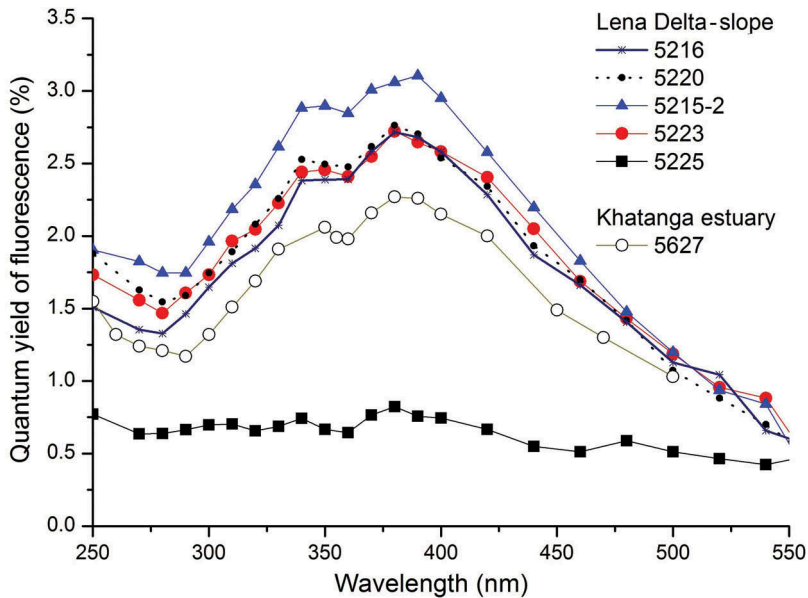


**Figure 6.** FQY of CDOM as a function of excitation wavelength for the surface seawater samples of the Laptev Sea (2015, 2017).

varies from 0.7% (station 5225, continental slope) to 2.9% (station 5215–2, water with minimal absorbance). Quantum yield of CDOM fluorescence from the Khatanga River estuary demonstrates similar dependence on excitation wavelength, while its values are lower (about 1.2 times at the maximum of FQY) for the whole wavelength range.

### 3.3. Kara Sea

Optical indices HIX, BIX, and  $S_R$  were calculated in order to supplement the information on DOM origin reported previously in (Drozdova, Patsaeva, and Khundzhua 2017). According to the data given in Table 2 DOM from the station 5199 is primarily of biological or aquatic bacterial origin. The rest DOM samples are characterized by important humic character and intermediate autochthonous component. Quantum yield of autochthonous DOM fluorescence (5199) at specific excitation wavelengths is about two times higher than the ones collected at the stations 5205 and 5214 and averaged 3.15%. FQY of two CDOM samples was described as a function of excitation wavelength, see Figure 7. The functions of FQY showed similar dependences on excitation wavelength. Two maxima are located around 340 nm and 380 nm and estimated as 2.13% and 2.31% for the CDOM from desalinated waters near the east coast of Novaya Zemlya archipelago (station 5205), 2.66% and 2.85% for the DOM sampled at the northern extremity of Novaya Zemlya (station 5214). In contrast to the previously discussed excitation-dependent FQY functions, its values from the station 5214 demonstrate a moderate increase at excitation wavelength 270 nm.

**Table 2.** FQY and optical indices of CDOM for the samples collected in the Kara and East Siberian seas. Salinity, HIX and BIX indices are published in (Drozdoва, Patsaeva, and Khundzhua 2017) and (Drozdoва, Krylov, and Shchuka 2018).

Sample	Salinity	FQY (%)			HIX	BIX	$a_{350}$ ( $m^{-1}$ )	$S_R$
		270 nm	310 nm	355 nm				
Kara Sea								
5199	31.7	3.14	3.40	2.92	2.12	0.89	0.7	1.50
5205	16.6	1.36	1.73	2.12	7.12	0.71	7.0	0.93
5214	28.2	1.70	2.12	2.62	6.14	0.74	5.3	1.01
The transect from the Kolyma River estuary to the continental slope								
5619	17.0	1.78	1.95	2.37	5.11	0.73	4.0	1.05
5615	28.1	1.71	2.01	2.52	1.53	0.94	0.5	1.71
5612	29.3	1.70	1.59	1.97	1.64	1.00	1.1	1.89
The transect from the Indigirka River estuary to the continental slope								
5598	15.1	1.89	2.08	2.60	3.74	0.84	4.7	1.07
5602	22.2	1.03	1.30	1.60	4.86	0.81	3.3	1.06
5607	30.0	0.74	0.77	1.01	1.38	1.02	2.0	1.92

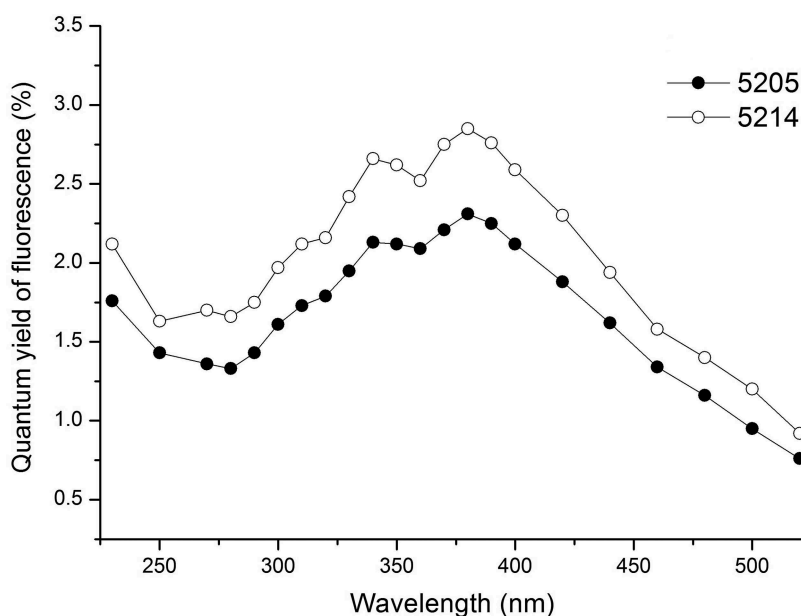


**Figure 7.** FQY of CDOM as a function of excitation wavelength for the surface seawater samples at the stations 5205 and 5214, Kara Sea (2015).

### 3.4. East Siberian Sea

$S_R$  values calculated from absorption spectra of six seawater samples from the East Siberian Sea vary from 1.05 to 1.92 proving the important autochthonous character of DOM. In accordance with BIX and HIX indices, given in Table 2, the contribution of terrigenous component was weak at the stations 5615 and 5612 at the transect from the Kolyma River estuary to the continental slope, and at the northern station at the transect starting from the Indigirka River estuary, 5607 (Huguet et al. 2009). The values of FQY of CDOM at excitation wavelengths 270, 310 and 355 nm are presented in Table 2. FQY dependencies of excitation wavelength (Figure 8) were evaluated for the surface waters

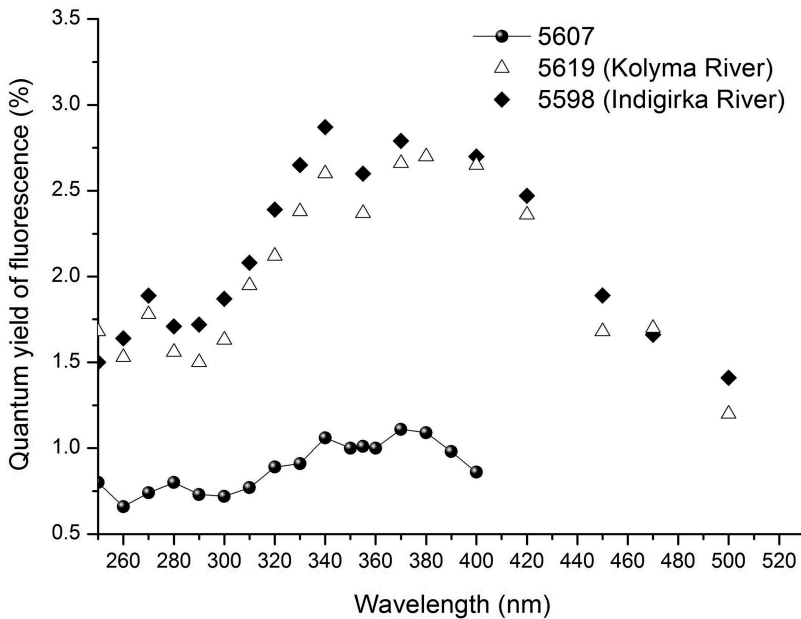


**Figure 8.** FQY of CDOM as a function of excitation wavelength for the surface seawater samples at the stations 5619 (waters influenced by the Kolyma River runoff), 5598 and 5607 (the transect from the Indigirka River to continental slope), East Siberian Sea (2017).

from the southmost stations of the transects most influenced by terrestrial environment, and also for the station 5607. Similarly to discussed above functions, the FQY dependence for the studied samples demonstrates two peaks at 340 and 380 nm, with constant further decrease towards longer excitation wavelengths. Also, an additional maximum at  $\lambda_{\text{ex}} = 270$  nm is observed for the samples 5598 and 5619. FQY of CDOM from the station 5607 did not show any pronounced extremes, its value varied from 0.6% to 1.11% for excitation wavelengths 250–400 nm.

## 4. Discussion

### 4.1. CDOM characterization

Absorption coefficient  $a_{350}$ ,  $S_{\text{UVB}}$ , and  $S_{\text{R}}$  values obtained for the White Sea surface waters agree well with the results reported in (Pavlov et al. 2016), taking into account that Pavlov and co-workers investigated the waters within salinity range 20.0–34.8. In the present study,  $S_{\text{UVB}}$  varies between 12.9 and 15.0  $\mu\text{m}^{-1}$  while in (Pavlov et al. 2016), this parameter was estimated as 14.5–28.5  $\mu\text{m}^{-1}$  with the lowest values of 14.5–17.0  $\mu\text{m}^{-1}$  typical for the waters in proximity of the Northern Dvina River. As anticipated, the highest  $a_{350}$  value of 13.7  $\text{m}^{-1}$  in (Pavlov et al. 2016) was observed for waters most strongly affected by the Northern Dvina River runoff (salinity 20.0) which is comparable with  $a_{350}$  of surface water at the station MF-3 (14.1  $\text{m}^{-1}$ ) with salinity 21.1. The spectral slope ratio values ( $0.78 < S_{\text{R}} < 0.88$ ) are also in agreement with the previously published results for the seawater samples with salinity below 30

( $0.75 < S_R < 1.00$ ) (Pavlov et al. 2016). Values of  $a_{350}$  for the surface waters of the East Siberian and Laptev seas varied between 0.5 and  $12.3 \text{ m}^{-1}$ , wherein the lowest absorption coefficient was measured at the station 5615 and amounted to  $0.5 \text{ m}^{-1}$  which is close to the ones reported for the Polar Waters of the East Greenland Current given in (Pavlov et al. 2015; Granskog et al. 2015). In the study of Pugach et al. (2018) a comparable spatial variability of  $a_{350}$  was demonstrated: it was reported to fall in the range  $0.7 < a_{350} < 17.3 \text{ m}^{-1}$ . Absorption coefficients of the East Siberian Sea surface waters, however, varied in a narrow range from 0.5 to  $4.7 \text{ m}^{-1}$  (see Table 2). Such  $a_{350}$  values are typical for the waters of the central and eastern Arctic Ocean (Gonçalves-Araujo et al. 2018) rather than for estuarine zones. Spectral slope ratios  $S_R$  obtained in the present study ( $0.93 < S_R < 1.92$ ) for the Laptev and East Siberian seas surface waters are generally consistent with the results of Pugach et al. (2018) ( $0.8 < S_R < 1.8$ ), but slightly higher at the utmost stations of the transects 5607 and 5612, least affected by terrestrial runoff. Within the transect along the  $130^\circ\text{E}$  in the Laptev Sea  $S_R$  amounted to 0.93–0.99, which agrees well with the data reported for seawaters in the Lena Delta region by Pugach et al. (0.92) (Pugach et al. 2015) and by Gonçalves-Araujo et al. ( $\sim 0.87$ – $1.00$ ) (Gonçalves-Araujo et al. 2015). A higher value,  $S_R = 1.07$ , was obtained for the seawater sample with salinity 30.1 collected at the northmost station 5225, where the influence of the Lena River runoff reduced significantly (Sukhanova et al. 2017; Stepanova, Polukhin, and Kostyleva 2017). The values of  $a_{350}$  measured for the Laptev Sea waters ( $2.1 < a_{350} < 12.3 \text{ m}^{-1}$ ) also agree with the data reported for the Lena Delta region in (Gonçalves-Araujo et al. 2015) ( $0.9 < a_{350} < 15.7 \text{ m}^{-1}$ ).

For most of the surface seawater samples from the Arctic shelf areas under investigation, namely, the White, Kara, Laptev, and East Siberian seas, the terrestrial-derived organic matter represented by humic substances was found to be a dominant component of CDOM. This is indicated by the spectral slope ratio  $S_R$  varying between 0.78 and 1.07 (Stedmon and Nelson 2015). For comparison,  $S_R$  values for river samples were reported to vary between seasons and estimated by Stedmon et al. (Stedmon et al. 2011) as 0.82–0.92 (Kolyma), 0.81–0.89 (Lena), 0.83–0.92 (Ob), and 0.79–0.93 (Yenisei). In our study, the lowest  $S_R$  values were measured for the desalinated waters of the White Sea influenced by the Northern Dvina River runoff, the highest ones – for the surface waters of the East Siberian Sea (above 1.05). Absorption spectra of the samples from the Kara Sea, influenced by Ob and Yenisei riverine waters, and from the Khatanga River estuary are characterized by spectral slope ratio  $S_R$  amounted to 0.93–1.01, HIX index 6.14–9.24, and BIX index 0.62–0.74, which testifies to the mixed autochthonous-allochthonous DOM character. Fewer DOM samples were found to be of freshly released biological origin (bacterial or planktonic) having strong autochthonous component and weak humic character. Low impact of riverine waters for the sample collected near Novaya Zemlya Trough in the Kara Sea (station 5199, salinity 31.7) approved by high  $S_R$  and BIX values (1.50 and 0.89, respectively) and low value of HIX = 2.12. Other three samples were taken in the East Siberian Sea at the stations 5607 ( $S_R = 1.92$ ), 5612 ( $S_R = 1.89$ ) and 5615 ( $S_R = 1.71$ ), located far to the north from the estuarine zones of the Indigirka and Kolyma rivers. Similar results were obtained by us on a basis of HIX and BIX indices reported in (Drozдова, Krylov, and Shchuka 2018).

#### 4.2. CDOM fluorescence quantum yield as a function of excitation wavelength within 240–500 nm

FQY of CDOM for 12 samples was described as a function of excitation wavelength in the range from 240 to 500–550 nm. In most cases, it was decreasing from excitation wavelength of 240 nm to 270–280 nm, and then it was rising exhibiting two peaks at 340 and 380 nm with further decrease towards longer excitation wavelengths. The maximum at 380 nm is more pronounced than at 340 nm with an exception of one sample (station 5598, East Siberian Sea, see Figure 9). Such behavior of FQY was observed for the surface waters from the Kara, Laptev and White seas, where the dominant contribution of terrestrial-derived HS was determined ( $S_R < 1.00$ ). These data on FQY are consistent with the results of investigations of terrestrial material and CDOM from coastal margins receiving terrestrial input discussed in (Green and Blough 1994; Andrew et al. 2013; Wünsch, Murphy, and Stedmon 2015; Cawley, Korak, and Rosario-Ortiz 2015; Zepp, Sheldon, and Moran 2004). Thus, in the study of Green and Blough (1994) a wavelength dependence of FQY of CDOM from marine, riverine, and estuarine waters from south Florida waters, the Amazon and the Tamiami rivers, and Suwannee River fulvic acid was found to be similar: the peak fluorescence efficiencies were obtained at excitation wavelengths between 380 and 400 nm. The samples also shared a distinct peak at 355 nm, and some spectra had a shoulder at 445–450 nm. FQY was estimated to be ~1% with small variation around this value, while absorption coefficients at  $\lambda_{ex} = 355$  nm varied in a wide range from 0.1 to 40  $m^{-1}$ . Investigation of

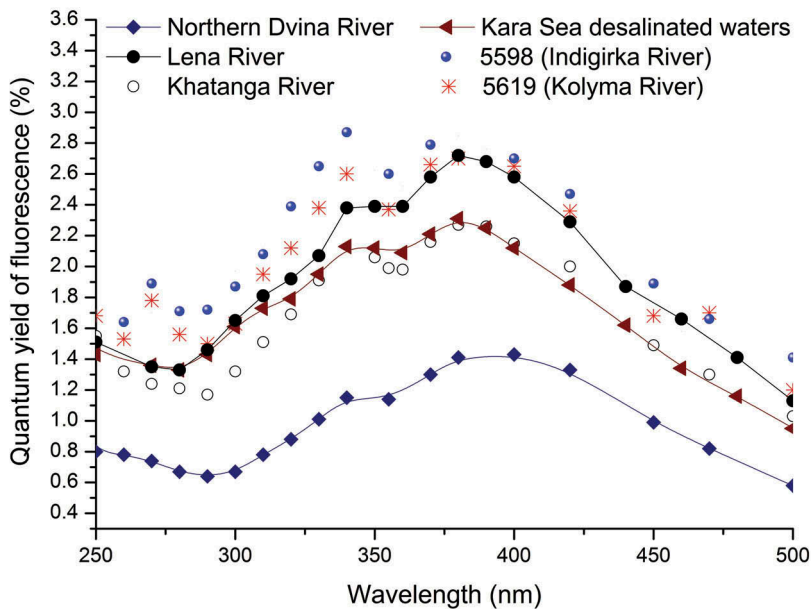


**Figure 9.** FQY of CDOM as a function of excitation wavelength for the surface seawater samples from the sites mostly affected by terrestrial runoff: riverine water of the Northern Dvina (MF-9,  $S_R = 0.78$ ), Lena Delta region (5216, salinity 3.0,  $S_R = 0.93$ ), Khatanga River estuary (5627, salinity 3.5,  $S_R = 1.00$ ), desalinated waters of the Kara (5205, salinity 16.6,  $S_R = 0.93$ ) and East Siberian (5598, salinity 15.1,  $S_R = 1.07$  and 5619, salinity 17.0,  $S_R = 1.05$ ) seas.



Suwannee River fulvic acid and Suwannee River humic acid published in (Del Vecchio and Blough 2004) has shown that FQY increased from  $\lambda_{\text{ex}}$  of 290 nm to a maximum at 350 nm, and then decreased monotonically with increasing of excitation wavelength. Later FQY of natural organic matter, the hydrophobic organic acid fraction, and the transphilic acid fraction from the Suwannee River was reported to exhibit similar behavior with two maxima around 340 and 370 nm (Cawley, Korak, and Rosario-Ortiz 2015). In the study of Andrew et al. (2013) spectral dependence of FQY was used as an evidence of the presence of terrestrial material in natural waters across the Equatorial Atlantic Ocean. FQY increased from 280 nm to a maximum at 370–380 nm ranging from 1.8% to 2.5% and decreased monotonically thereafter. Additional maximum at  $\sim 340$  nm was observed for CDOM from a site influenced by the Congo River Plume. Distinct emission bands in the ultraviolet were supposed to cause significantly higher values of CDOM FQY of 5–7%. FQY of deep and surface waters of the Norwegian Sea (Wünsch, Murphy, and Stedmon 2015) also demonstrated similar behavior with minima around 250 nm increasing to maxima between 340 and 380 nm. FQY values at excitation wavelength 350 nm ranged from 0.6% to 2.1%. FQY of CDOM in surface waters was found to be significantly lower than in deep-sea waters, on average equals to  $1.4 \pm 0.3\%$ . Investigation of the FQY of CDOM samples with salinities 0.2–34.6 collected at the transect along the Satilla River (USA) was performed by Zepp, Sheldon, and Moran (2004). FQY increased with increasing salinity and pH in the estuary. The highest quantum yields were observed on excitation by 350–380-nm light.

For the seawater samples from the East Siberian Sea an additional maximum at excitation wavelength  $\sim 270$  nm was observed and the maximum at 340 nm became better resolved (Figure 9). In the Kara Sea, similar behavior was detected for the seawater sample from the station 5214 located in the region of the St. Anna Trough (Figure 7). All the CDOM samples showing such an increase of FQY at an excitation wavelength of  $\sim 270$  nm are characterized by the slope ratio  $1.0 < S_R < 1.07$ . This feature of FQY function is due to an increase of protein-like fluorescence contributing into overall fluorescence intensity excited at 270–280 nm (Coble et al. 2014). Once again we emphasize that protein-like fluorescence with maximum around 300–350 nm not necessarily is caused by proteinous material, but could be resulted from derivatives of aromatic amino-acids and phenols (Patsayeva and Reuter 1995; Trubetskaya, Richard, and Trubetskoj 2016). In any case, its appearance is an indication of the presence of labile biological material in studied waters.

FQY of CDOM was found to be very low for water from the station 5607, it did not exceed a percent and did not reveal any pronounced extrema (Figure 8). Similarly, the seawater from the station 5225 showed about 5 times lower values at the maximum of FQY compared to the shelf region and no variation with excitation wavelength (Figure 6). In both cases, the dropping of the FQY is due to the decrease in the humic-like fluorescence intensity of CDOM far from mixing zones of the Lena and Indigirka rivers. Maximal FQY (measured at  $\lambda_{\text{ex}} = 380$  nm) of CDOM for the waters influenced by terrestrial-derived organic matter varied from 1.43% to 2.85% at the White Sea surface waters, affected by the Northern Dvina River runoff, are characterized by the lowest FQY. Its value at 355 nm fell in a range between 1.13% and 1.65%. These results agree well with the data obtained for the surface waters of the Norwegian Sea ( $1.4 \pm 0.3\%$ ) (Wünsch, Murphy, and Stedmon 2015), South Florida waters (0.8–1.5%)

(Green and Blough 1994), and the waters from Satilla River (0.8–1.4%) (Wünsch, Murphy, and Stedmon 2015). Slightly larger FQY values were obtained for the East Siberian Sea waters influenced by the Khatanga River freshwater (1.72%). In case of the rest studied areas FQY was significantly higher and estimated on the average as 2.56% for the Laptev Sea surface waters (the Lena River Plume), 2.37% for the Kara Sea, and 2.21% for the East Siberian Sea (except the station 5607). Similar FQY (1.8–2.5%) was measured in the Equatorial Atlantic Ocean water composed of a major terrestrial component (Andrew et al. 2013).

The interpretation of FQY dependencies is challenging since CDOM represents a class of complex molecular structures, naturally formed by transformation and assemblage processes of biomolecules originating from microbial, plant and animal residues (Weber et al. 2018). Therefore, the exact composition of fluorophores is not known. All techniques of chromatographic CDOM separation give fluorescing fractions, though with varying emission efficiency. Moreover, CDOM fractionation helps to reveal CDOM fractions with protein-like fluorescence even for those freshwater samples which do not demonstrate protein-like fluorescence on whole CDOM (Patsaeva et al. 2018). In some cases, FQY is not a merely characteristic of chromophoric/fluorescent DOM pool size, but reflects also the chromophores interaction. However, this topic does not fall within the scopes of the current paper.

#### **4.3. Evolution of CDOM fluorescence quantum yield along the salinity gradient**

In case of the White Sea surface waters, affected by the Northern Dvina River runoff, we observed a conservative behavior of CDOM at salinities from 0 to 24.5. This is indicated by a linear correlation  $a_{350} - \text{Salinity}$  (see Figure 3), while  $a_{350}$  was reported to be better suited to quantify dissolved organic carbon (Walker, Amon, and Stedmon 2013). An apparent increase of FQY at each of the studied excitation wavelength with the increase of salinity was observed, see Figure 5. It grew up from 0.73% to 1.20% at  $\lambda_{\text{ex}} = 270$  nm, from 0.77% to 1.32% at  $\lambda_{\text{ex}} = 310$  nm and from 1.13% to 1.65% at  $\lambda_{\text{ex}} = 355$  nm. Positive correlations between FQY and salinity can be related to a number of reasons: the changing CDOM composition along the transect; reduce of fluorescence quenching due to the decrease of CDOM concentration; finally, the lower values of FQY of riverine CDOM samples can be associated with the presence of fluorescence quenchers in river water, concentration of which decreases with the distance from the estuarine zone. To reveal the influence of CDOM quality on FQY, the SUVA index was analyzed. An example of the Laptev Sea surface waters indicates that the change of SUVA by  $0.11 \text{ m}^2\text{gC}^{-1}$ , which corresponds to the variations in percent aromaticity of 19.3–20.1% (Weishaar et al. 2003) along the salinity gradient 3.0–22.2, does not affect FQYs significantly, see Figure 6. Similar changes in CDOM aromaticity was observed, for example, for the stations MF5–MF8. FQYs, however, demonstrated a positive correlation with salinity. Taking into account the large DOC concentrations in the delta region of the Northern Dvina River (DOC at the station MF9 accounted to 22.5 mg/L), we assume that the positive correlation FQY – salinity at low salinity values is most likely caused by the decrease of collisional quenching of fluorescence. At higher salinities, both fluorescence quenching and the change of CDOM composition may affect the FQY values.

Another area where the change of CDOM fluorescence quantum yield was studied along the salinity gradient is the Laptev Sea. FQY of the Laptev Sea surface waters remained constant with the increase of salinity from 3.0 to 20.6 (see the data for the stations 5216, 5220 and 5223 in Table 1). The exception is the station 5215–2, where CDOM has higher values (2.9% at 355 nm) of FQY, see Figure 6. According to the data reported in (Sukhanova et al. 2017; Stepanova, Polukhin, and Kostyleva 2017), the pycnocline at this site locally rises to the surface. This is consistent with the results of Ferrari (2000) and Wünsch, Murphy, and Stedmon (2015), who stated that upper Mediterranean waters (upwelling) as well as the deep waters of Norwegian Sea and at the summit of the seamounts of the Atlantic are characterized by higher FQY compared with surface waters. Compared to other stations, abnormal nutrient distribution was observed in the surface layer at this location, for example, an increased total and nitrate nitrogen contents, low ammonium nitrogen values, and higher total alkalinity values. At the same time, the greatest contribution of autochthonous component was observed while maintaining the dominant role of terrigenous organic matter. The change in FQY may be associated with both the change in the composition of organic matter and hydrochemical parameters altered dramatically at that location. The latter being most likely: spectral slope  $S_R$  for the samples from stations 5216, 5220, and 5223 varies between 0.93 and 0.97, which did not affect FQY function significantly, so, further increase of contribution of autochthonous OM, resulted in increase of  $S_R$  up to 0.99, can hardly cause an increase of the quantum yield of CDOM fluorescence observed at the station 5215–2.

## 5. Conclusions

Along with traditional optical indices, calculated from absorption and fluorescence spectra to describe CDOM naturally occurring in water, the correlations between CDOM fluorescence and absorption, known as apparent fluorescence quantum yield becomes significant. Knowledge of CDOM optical properties through different wavelengths ranges is important for satellite remote sensing as well as for lidar ground-true measurements. Therefore, the aim of this research was to improve our understanding of the traditional optical indices and the FQY measured at different excitations in the context of variable hydrological conditions in the Arctic. We have examined the FQY as a function of excitation wavelength for a variety of the Arctic shelf areas affected by freshwater runoff. Similar wavelength-dependent behavior of FQY was established for various samples: it was decreasing from excitation wavelength of 240 nm to 270–280 nm, and then it was rising, exhibiting two peaks at roughly 340 and 380 nm, with further decrease towards longer excitation wavelengths. Generally, one can expect that the change in CDOM composition leads to the alteration of FQY function through both fluorescent and absorption characteristics of CDOM. For example, in the present study distinctive features of CDOM with strong humic character, but significant contribution of labile autochthonous organic matter, were represented by appearance of the additional maximum at excitation wavelength ~270 nm, as well as a better resolution of the FQY peak at ~340 nm, which was observed for the surface waters of the East Siberian Sea. Detection of different components of CDOM, such as fulvic acids, high molecular weight and aromatic humic, etc., with the use of FQY function is less

straightforward: according to Fellman, Hood, and Spencer (2010), the difference in position of fluorescence band maxima of various fluorophores may not exceed 10–20 nm, or even overlap with each other. So, for further investigations of FQY as a potential marker of biochemical processes, we would suggest to measure FQY as a function of excitation wavelength with higher resolution and correlate the form of FQY functions with optical indices or concentration of PARAFAC components.

Apart from the form of wavelength-dependence of FQY, its absolute value is an important characteristic of natural waters. In the present study, it was demonstrated, that FQY of the surface waters under investigation at excitation wavelength 355 nm varied in a range from 0.67% at the continental slope region of the Laptev Sea to 2.62% in the Kara Sea. The average values of FQY of the studied samples are summarized in Table 3. If the composition of CDOM does not vary within a set of samples, FQY will remain constant (Stedmon and Nelson 2015). An example of such an FQY behaviour was observed for the Laptev Sea surface waters influenced by the Lena River runoff: FQY functions are the same within the range of studied excitation wavelengths and the salinity gradient. A higher value of FQY was measured for the surface CDOM in the location, where deep waters in the Laptev Sea are coming to the surface (upwelling). Compared to absorption and fluorescence spectra, FQY demonstrates the similarity of CDOM composition more clearly in both freshwater and marine environment, since it does not depend on the concentration of fluorophores. We showed, however, that collisional quenching of fluorescence, especially for the humic substances of higher molecular weight, can affect FQY in estuarine zones. Thus, for the seawater samples from the White Sea, demonstrating conservative mixing of the terrestrial DOM, the FQY values were linearly growing along with salinity. Composition of CDOM did not change significantly at salinities below 10.5. At higher salinities both the change in the ratio of autochthonous to allochthonous components and collisional fluorescence quenching may take place, so additional laboratory experiments would be beneficial to reveal the concentration/ $a_{350}$  range, for which relaxation processes are significant. Furthermore, collisional quenching of fluorescence may be caused by molecular oxygen (Lakowicz 2006), so the data on oxygen concentration under the conditions of the detection of spectra or a procedure, providing an O<sub>2</sub> equilibrium between atmosphere and a sea-water sample, might be useful.

Finally, interpretation of FQY of natural water is not straightforward, since it depends on CDOM quality and composition of the studied waters, including inorganic components. For the same reason, it represents a more informative characteristic of natural waters. For example, FQY has a potential to reveal the areas of the Laptev Sea affected by the Khatanga and Lena waters, having similar spectral features, due to significant difference in FQY meanings, 1.72% and 2.56%, respectively.

**Table 3.** Fluorescence quantum yield at excitation wavelength of 355 nm for the surface seawater samples of the White, Kara, Laptev and East Siberian seas influenced by freshwater runoff. Number of samples is given in brackets.

FQY(355)	White Sea	Kara Sea	Laptev Sea		East Siberian Sea
	Northern Dvina (9)	Ob and Yenisei (2)	Khatanga (2)	Lena (4)	Indigirka and Kolyma (5)
Range (%)	1.13–1.65	2.12–2.62	1.69–1.74	2.39–2.90	1.60–2.60
Average (%)	1.44	2.55	1.72	2.56	2.21

## Acknowledgments

The researches in the Siberian Arctic seas were performed in the framework of the state assignment of FASO Russia (theme No. 0149-2018-0005). The study of the Laptev and Kara seas optical properties was funded by RFBR, according to the research project No. 16-35-60032 mol\_a\_dk. The calculations of fluorescence quantum yield were funded by RFBR research project No. 18-016-00078. The authors thank A.I. Kochenkova, N.M. Mahnovich, and A.S. Lohov and the crew of the RV *Akademik Mstislav Keldysh* for their assistance in the fieldworks.

## Disclosure statement

No potential conflict of interest was reported by the authors.

## Funding

This work was supported by the Federal Agency for Scientific Organizations [0149-2018-0005]; Russian Foundation for Basic Research [16-35-60032 mol\_a\_dk, 18-016-00078];

## ORCID

Anastasia N. Drozdova  <http://orcid.org/0000-0002-5547-6693>

## References

- Amon, R. M. W. 2004. "The Role of Dissolved Organic Matter for the Organic Carbon Cycle in the Arctic Ocean." In *The Organic Carbon Cycle in the Arctic Ocean*, edited by R. Stein and R. W. Macdonald, 83–99. Berlin: Springer-Verlag Berlin Heidelberg.
- Andrew, A. A., R. Del Vecchio, A. Subramaniam, and N. V. Blough. 2013. "Chromophoric Dissolved Organic Matter (CDOM) in the Equatorial Atlantic Ocean: Optical Properties and Their Relation to CDOM Structure and Source." *Marine Chemistry* 148: 33–43. doi:10.1016/j.marchem.2012.11.001.
- Belin, C., C. Quéllec, M. Lamotte, M. Ewald, and P. Simon. 1993. "Characterization by Fluorescence of the Dissolved Organic-Matter in Natural-Water - Application to Fractions Obtained by Tangential Ultrafiltration and Xad Resin Isolation." *Environmental Technology* 14 (12): 1131–1144. doi:10.1080/09593339309385391.
- Cawley, K. M., J. A. Korak, and F. L. Rosario-Ortiz. 2015. "Quantum Yields for the Formation of Reactive Intermediates from Dissolved Organic Matter Samples from the Suwannee River." *Environmental Engineering Science* 32 (1): 31–37. doi:10.1089/ees.2014.0280.
- Chekalyuk, A., and M. Hafez. 2013. "Next Generation Advanced Laser Fluorometry (ALF) for Characterization of Natural Aquatic Environments: New Instruments." *Optics Express* 21 (12): 14181–14201.
- Coble, P. G. 2007. "Marine Optical Biogeochemistry: The Chemistry of Ocean Color." *Chemical Reviews* 107 (2): 402–418. doi:10.1021/cr050350+.
- Coble, P. G., R. G. M. Spencer, A. Baker, and D. M. Reynolds. 2014. "Aquatic Organic Matter Fluorescence." *Aquatic Organic Matter Fluorescence* 75–122. doi:10.1017/Cbo9781139045452.
- David, M. A., L. G. Anderson, T. R. Christensen, S. Dallimore, D. J. Laodong Guo, M. H. Hayes, T. D. Lorenson, R. W. Macdonald, and N. Roulet. 2009. "Sensitivity of the Carbon Cycle in the Arctic to Climate Change." *Ecological Monographs* 79 (4): 523–555. doi:10.1890/08-2025.1.
- Del Vecchio, R., and N. V. Blough. 2004. "On the Origin of the Optical Properties of Humic Substances." *Environmental Science & Technology* 38 (14): 3885–3891. doi:10.1021/es049912h.

- Drozdova, A. N., I. N. Krylov, and S. A. Shchuka. 2018. "CDOM Fluorescence of the Laptev Sea and East Siberean Sea Surface Waters." *EARSeL eProceedings* 17 (1): 1–6. doi:10.12760/01-2018-1-01.
- Drozdova, A. N., S. V. Patsaeva, and D. A. Khundzhua. 2017. "Fluorescence of Dissolved Organic Matter as a Marker for Distribution of Desalinated Waters in the Kara Sea and Bays of Novaya Zemlya Archipelago." *Oceanology* 57 (1): 41–47. doi:10.1134/S0001437017010039.
- Fantoni, R., R. Barbini, F. Colao, D. Ferrante, L. Fiorani, and A. Palucci. 2004. "INTEGRATION of TWO LIDAR FLUOROSENSOR PAYLOADS in SUBMARINE ROV and FLYING UAV PLATFORMS." *EARSeL eProceedings* 3 (1): 43.
- Fellman, J. B., E. Hood, and R. G. M. Spencer. 2010. "Fluorescence Spectroscopy Opens New Windows into Dissolved Organic Matter Dynamics in Freshwater Ecosystems: A Review." *Limnology and Oceanography* 55 (6): 2452–2462. doi:10.4319/lo.2010.55.6.2452.
- Ferrari, G. M. 2000. "The Relationship between Chromophoric Dissolved Organic Matter and Dissolved Organic Carbon in the European Atlantic Coastal Area and in the West Mediterranean Sea (Gulf of Lions)." *Marine Chemistry* 70 (4): 339–357. doi:10.1016/S0304-4203(00)00036-0.
- Gonçalves-Araujo, R., B. Rabe, I. Peeken, and A. Bracher. 2018. "High Colored Dissolved Organic Matter (CDOM) Absorption in Surface Waters of the Central-Eastern Arctic Ocean: Implications for Biogeochemistry and Ocean Color Algorithms." *PloS One* 13 (1): e0190838. doi:10.1371/journal.pone.0190838.
- Gonçalves-Araujo, R., C. A. Stedmon, B. Heim, I. Dubinenkov, A. Kraberg, D. Moiseev, and A. Bracher. 2015. "From Fresh to Marine Waters: Characterization and Fate of Dissolved Organic Matter in the Lena River Delta Region, Siberia." *Frontiers in Marine Science* 2. doi:10.3389/fmars.2015.00108.
- Gorshkova, O. M., A. S. Milukov, S. V. Patsayeva, and V. I. Yuzhakov. 2005. "Fluorescence of DOM Nanoparticles in Natural Water - Art. No. 62630Y." *Atomic and Molecular Pulsed Lasers VI* 6263: Y2630–Y. doi:10.1117/12.677453.
- Gosteva, O. Y., A. A. Izosimov, S. V. Patsaeva, V. I. Yuzhakov, and O. S. Yakimenko. 2012. "Fluorescence of Aqueous Solutions of Commercial Humic Products." *Journal of Applied Spectroscopy* 78 (6): 884–891. doi:10.1007/s10812-012-9548-8.
- Granskog, M. A., A. K. Pavlov, S. Sagan, P. Kowalczyk, A. Raczkowska, and C. A. Stedmon. 2015. "Effect of Sea-Ice Melt on Inherent Optical Properties and Vertical Distribution of Solar Radiant Heating in Arctic Surface Waters." *Journal of Geophysical Research: Oceans* 120 (10): 7028–7039. doi:10.1002/2015JC011087.
- Green, S. A., and N. V. Blough. 1994. "Optical-Absorption and Fluorescence Properties of Chromophoric Dissolved Organic-Matter in Natural-Waters." *Limnology and Oceanography* 39 (8): 1903–1916. doi:10.4319/lo.1994.39.8.1903.
- Grunwald, M., O. Dellwig, G. Liebezeit, B. Schnetger, R. Reuter, and H. J. Brumsack. 2007. "A Novel Time-Series Station in the Wadden Sea (NW Germany): First Results on Continuous Nutrient and Methane Measurements." *Marine Chemistry* 107 (3): 411–421. doi:10.1016/j.marchem.2007.04.003.
- Harsdorf, S., M. Janssen, R. Reuter, S. Toeneboen, B. Wachowicz, and R. Willkomm. 1999. "Submarine Lidar for Seafloor Inspection." *Measurement Science and Technology* 10 (12): 1178–1184. doi:10.1088/0957-0233/10/12/309.
- Hawes, S. K., K. L. Carder, and G. R. Harvey. 1992. "Quantum Fluorescence Efficiencies of Fulvic and Humic Acids: Effects on Ocean Color and Fluorometric Detection." In *Proc. SPIE, Ocean Optics XI*, Vol. 1750, edited by G. D. Gilbert, 212–224. Bellingham: International Society for Optics and Photonics. doi:10.1117/12.140652.
- Helms, J. R., A. Stubbins, J. D. Ritchie, E. C. Minor, D. J. Kieber, and K. Mopper. 2008. "Absorption Spectral Slopes and Slope Ratios as Indicators of Molecular Weight, Source, and Photobleaching of Chromophoric Dissolved Organic Matter." *Limnology and Oceanography* 53 (3): 955–969. doi:10.4319/lo.2008.53.3.0955.
- Hockaday, W. C., J. M. Purcell, A. G. Marshall, J. A. Baldock, and P. G. Hatcher. 2009. "Electrospray and Photoionization Mass Spectrometry for the Characterization of Organic Matter in Natural

- Waters: A Qualitative Assessment." *Limnology and Oceanography: Methods* 7 (1): 81–95. doi:10.4319/lom.2009.7.81.
- Huguet, A., L. Vacher, S. Relexans, S. Saubusse, J. M. Froidefond, and E. Parlanti. 2009. "Properties of Fluorescent Dissolved Organic Matter in the Gironde Estuary." *Organic Geochemistry* 40 (6): 706–719. doi:10.1016/j.orggeochem.2009.03.002.
- Khundzhua, D. A., S. V. Patsaeva, O. A. Trubetskoj, and O. E. Trubetskaya. 2017. "An Analysis of Dissolved Organic Matter from Freshwater Karelian Lakes Using Reversed-Phase High-Performance Liquid Chromatography with Online Absorbance and Fluorescence Analysis." *Moscow University Physics Bulletin* 72 (1): 68–75. doi:10.3103/S002713491701009x.
- Kochenkova, A. I., A. N. Novigatskiy, and V. V. Gordeev. 2018. "Distribution of Suspended Matter in the Marginal Filter of the Northern Dvina at the End of Summer." *Modern Problems of Science and Education* 2: 106–112. (in Russian). doi:10.17513/use.36680.
- Kostianoy, A. G., and J. C. J. Nihoul. 2009. "Frontal Zones in the Norwegian, Greenland, Barents and Bering Seas." In *Influence of Climate Change on the Changing Arctic and Sub-Arctic Conditions*, edited by J. C. J. Nihoul and A.G. Kostianoy, 171–190. Dordrecht: Springer.
- Kutser, T., B. Paavel, L. Metsamaa, and E. Vahtmae. 2009. "Mapping Coloured Dissolved Organic Matter Concentration in Coastal Waters." *International Journal of Remote Sensing* 30 (22): 5843–5849. doi:10.1080/01431160902744837.
- Lakowicz, J. R. 2006. *Principles of Fluorescence Spectroscopy*. Berlin: Springer.
- Leenheer, J. A., and J. P. Croue. 2003. "Characterizing Aquatic Dissolved Organic Matter." *Environmental Science & Technology* 37 (1): 18a–26a. doi:10.1021/es032333c.
- Lobbis, J. M., H. P. Fitznar, and G. Kattner. 2000. "Biogeochemical Characteristics of Dissolved and Particulate Organic Matter in Russian Rivers Entering the Arctic Ocean." *Geochimica Et Cosmochimica Acta* 64 (17): 2973–2983. doi:10.1016/S0016-7037(00)00409-9.
- Lubben, A., O. Dellwig, S. Koch, M. Beck, T. Badewien, S. Fischer, and R. Reuter. 2009. "Distributions and Characteristics of Dissolved Organic Matter in Temperate Coastal Waters (Southern North Sea)." *Ocean Dynamics* 59 (2): 263–275. doi:10.1007/s10236-009-0181-x.
- Makkaveev, P. N., A. A. Polukhin, A. V. Kostyleva, E. A. Protsenko, S. V. Stepanova, and S. K. Yakubov. 2017. "Hydrochemical Features of the Kara Sea Aquatic Area in Summer 2015." *Oceanology* 57 (1): 48–57. doi:10.1134/S0001437017010088.
- Mann, P. J., G. M. Robert, P. J. Spencer, J. S. Hernes, G. R. Aiken, S. E. Tank, J. W. McClelland, K. D. Butler, R. Y. Dyda, and R. M. Holmes. 2016. "Pan-Arctic Trends in Terrestrial Dissolved Organic Matter from Optical Measurements." *Frontiers in Earth Science* 4: 25. doi:10.3389/feart.2016.00025.
- Mannino, A., M. G. Novak, S. B. Hooker, K. Hyde, and D. Aurin. 2014. "Algorithm Development and Validation of CDOM Properties for Estuarine and Continental Shelf Waters along the Northeastern U.S. Coast." *Remote Sensing of Environment* 152: 576–602. doi:10.1016/j.rse.2014.06.027.
- Marshall, A. G., C. L. Hendrickson, and G. S. Jackson. 1998. "Fourier Transform Ion Cyclotron Resonance Mass Spectrometry: A Primer." *Mass Spectrometry Reviews* 17 (1): 1–35. doi:10.1002/(sici)1098-2787(1998)17:1<1::Aid-mas1>3.0.Co;2-k.
- Meier, W. N., G. K. Hovelsrud, E. H. Bob, J. R. Van Oort, K. M. Key, C. M. Kovacs, C. Haas, et al. 2014. "Arctic Sea Ice in Transformation: A Review of Recent Observed Changes and Impacts on Biology and Human Activity." *Reviews of Geophysics* 52 (3): 185–217. doi:10.1002/2013rg000431.
- Milyukov, A. S., S. V. Patsaeva, V. I. Yuzhakov, O. M. Gorshkova, and E. M. Prashchikina. 2007. "Fluorescence of Nanoparticles of Organic Matter Dissolved in Natural Water." *Moscow University Physics Bulletin* 62 (6): 368–372. doi:10.3103/s0027134907060082.
- Orek, H., R. Doerffer, R. Rottgers, M. Boersma, and K. H. Wiltshire. 2013. "Contribution to a Bio-Optical Model for Remote Sensing of Lena River Water." *Biogeosciences* 10 (11): 7081–7094. doi:10.5194/bg-10-7081-2013.
- Palmer, S. C. J., V. V. Pelevin, I. Goncharenko, A. W. Kovacs, A. Zlinszky, M. Presing, H. Horvath, V. Nicolas-Perea, H. Balzter, and V. R. Toth. 2013. "Ultraviolet Fluorescence LiDAR (UFL) as a Measurement Tool for Water Quality Parameters in Turbid Lake Conditions." *Remote Sensing* 5 (9): 4405–4422. doi:10.3390/rs5094405.

- Parlanti, E., B. Morin, and L. Vacher. 2002. "Combined 3d-Spectrofluorometry, High Performance Liquid Chromatography and Capillary Electrophoresis for the Characterization of Dissolved Organic Matter in Natural Waters." *Organic Geochemistry* 33 (3): 221–236. doi:10.1016/S0146-6380(01)00154-1.
- Patsaeva, S., D. Khundzhua, O. A. Trubetskoj, and O. E. Trubetskaya. 2018. "Excitation-Dependent Fluorescence Quantum Yield for Freshwater Chromophoric Dissolved Organic Matter from Northern Russian Lakes." *Journal of Spectroscopy* 2018 (3168320): 1–7. doi:10.1155/2018/3168320.
- Patsayeva, S., and R. Reuter. 1995. "Spectroscopic Study of Major Components of Dissolved Organic Matter Naturally Occurring in Water." *Global Process Monitoring and Remote Sensing of the Ocean and Sea Ice* 2586: 151–160. doi:10.1117/12.228618.
- Pavlov, A. K., M. A. Granskog, C. A. Stedmon, B. V. Ivanov, S. R. Hudson, and S. Falk-Petersen. 2015. "Contrasting Optical Properties of Surface Waters across the Fram Strait and Its Potential Biological Implications." *Journal of Marine Systems* 143: 62–72. doi:10.1016/j.jmarsys.2014.11.001.
- Pavlov, A. K., C. A. Stedmon, A. V. Semushin, T. Martma, B. V. Ivanov, P. Kowalczyk, and M. A. Granskog. 2016. "Linkages between the Circulation and Distribution of Dissolved Organic Matter in the White Sea, Arctic Ocean." *Continental Shelf Research* 119: 1–13. doi:10.1016/j.csr.2016.03.004.
- Pelevin, V., A. Zlinszky, E. Khimchenko, and V. Toth. 2017. "Ground Truth Data on Chlorophyll-A, Chromophoric Dissolved Organic Matter and Suspended Sediment Concentrations in the Upper Water Layer as Obtained by LIF Lidar at High Spatial Resolution." *International Journal of Remote Sensing* 38 (7): 1967–1982. doi:10.1080/01431161.2016.1274446.
- Pugach, S. P., I. I. Pipko, I. P. Semiletov, and V. I. Sergienko. 2015. "Optical Characteristics of the Colored Dissolved Organic Matter on the East Siberian Shelf." *Doklady Earth Sciences* 465 (2): 1293–1296. doi:10.1134/S1028334x15120120.
- Pugach, S. P., I. I. Pipko, N. E. Shakhova, E. A. Shirshin, I. V. Perminova, Ö. Gustafsson, V. G. Bondur, A. S. Ruban, and I. P. Semiletov. 2018. "Dissolved Organic Matter and Its Optical Characteristics in the Laptev and East Siberian Seas: Spatial Distribution and Interannual Variability (2003–2011)." *Ocean Science* 14 (1): 87–103. doi:10.5194/os-14-87-2018.
- Raymond, P. A., J. W. McClelland, R. M. Holmes, A. V. Zhulidov, K. Mull, B. J. Peterson, R. G. Striegl, G. R. Aiken, and T. Y. Gurtovaya. 2007. "Flux and Age of Dissolved Organic Carbon Exported to the Arctic Ocean: A Carbon Isotopic Study of the Five Largest Arctic Rivers." *Global Biogeochemical Cycles* 21: 4. doi:10.1029/2007gb002934.
- Shubina, D., E. Fedoseeva, O. Gorshkova, S. Patsaeva, V. Terekhova, M. Timofeev, and V. Yuzhakov. 2010. "The "Blue Shift" of Emission Maximum and the Fluorescence Quantum Yield as Quantitative Spectral Characteristics of Dissolved Humic Substances." *EARSeL eProceedings* 9 (1): 13–21.
- Stedmon, C. A., R. M. W. Amon, A. J. Rinehart, and S. A. Walker. 2011. "The Supply and Characteristics of Colored Dissolved Organic Matter (CDOM) in the Arctic Ocean: Pan Arctic Trends and Differences." *Marine Chemistry* 124 (1–4): 108–118. doi:10.1016/j.marchem.2010.12.007.
- Stedmon, C. A., S. Markager, and R. Bro. 2003. "Tracing Dissolved Organic Matter in Aquatic Environments Using a New Approach to Fluorescence Spectroscopy." *Marine Chemistry* 82 (3–4): 239–254. doi:10.1016/S0304-4203(03)00072-0.
- Stedmon, C. A., S. Markager, and H. Kaas. 2000. "Optical Properties and Signatures of Chromophoric Dissolved Organic Matter (CDOM) in Danish Coastal Waters." *Estuarine Coastal and Shelf Science* 51 (2): 267–278. doi:10.1006/ecss.2000.0645.
- Stedmon, C. A., and N. B. Nelson. 2015. "The Optical Properties of DOM in the Ocean." In *Biogeochemistry of Marine Dissolved Organic Matter*, edited by D. A. Hansell and C. A. Carlson, 2nd ed. 481–508. Oxford: Academic Press.
- Stepanova, S. V., A. A. Polukhin, and A. V. Kostyleva. 2017. "Hydrochemical Structure of the Waters in the Eastern Part of the Laptev Sea in Autumn 2015." *Oceanology* 57 (1): 58–64. doi:10.1134/S0001437017010180.



- Sukhanova, I. N., M. V. Flint, E. J. Georgieva, E. K. Lange, M. D. Kravchishina, A. B. Demidov, A. A. Nedospasov, and A. A. Polukhin. 2017. "The Structure of Phytoplankton Communities in the Eastern Part of the Laptev Sea." *Oceanology* 57 (1): 75–90. doi:10.1134/S0001437017010209.
- Thurman, E. M. 2012. *Organic Geochemistry of Natural Waters*. Vol. 2. Berlin: Springer Science & Business Media.
- Trubetskaya, O. E., C. Richard, and O. A. Trubetskoj. 2015. "Evaluation of Suwannee River NOM Electrophoretic Fractions by RP-HPLC with Online Absorbance and Fluorescence Detection." *Environmental Science and Pollution Research* 22 (13): 9989–9998. doi:10.1007/s11356-015-4188-1.
- Trubetskaya, O. E., C. Richard, and O. A. Trubetskoj. 2016. "High Amounts of Free Aromatic Amino Acids in the Protein-Like Fluorescence of Water-Dissolved Organic Matter." *Environmental Chemistry Letters* 14 (4): 495–500. doi:10.1007/s10311-016-0556-4.
- Trubetskoi, O. A., and O. E. Trubetskaya. 2004. "Comparative Electrophoretic Analysis of Humic Substances in Soils and River and Lake Waters." *Eurasian Soil Science* 37 (11): 1170–1172.
- Trubetskoj, O. A., O. E. Trubetskaya, and C. Richard. 2009. "Photochemical Activity and Fluorescence of Electrophoretic Fractions of Aquatic Humic Matter." *Water Resources* 36 (5): 518–524. doi:10.1134/S0097807809050042.
- Velapoldi, R. A., and K. D. Mielenz. 1981. "A Fluorescence Standard Reference Material - Quinine Sulfate Dihydrate." *Applied Optics* 20 (9): 1718. doi:10.1364/Ao.20.001718.
- Vetrov, A. A., and E. A. Romankevich. 2004. *Carbon Cycle in the Russian Arctic Seas*. Berlin: Springer-Verlag Berlin Heidelberg.
- Walker, S. A., R. M. W. Amon, and C. A. Stedmon. 2013. "Variations in High-Latitude Riverine Fluorescent Dissolved Organic Matter: A Comparison of Large Arctic Rivers." *Journal of Geophysical Research-Biogeosciences* 118 (4): 1689–1702. doi:10.1002/2013jg002320.
- Weber, J., Y. Chen, E. Jamroz, and T. Miano. 2018. "Preface: Humic Substances in the Environment." *Journal of Soils and Sediments*. doi:10.1007/s11368-018-2052-x.
- Weishaar, J. L., G. R. Aiken, B. A. Bergamaschi, M. S. Fram, R. Fujii, and K. Mopper. 2003. "Evaluation of Specific Ultraviolet Absorbance as an Indicator of the Chemical Composition and Reactivity of Dissolved Organic Carbon." *Environmental Science & Technology* 37: 4702–4708. doi:10.1021/es030360x.
- Wünsch, U. J., B. P. Koch, M. Witt, and J. A. Needoba. 2016. "Seasonal Variability of Dissolved Organic Matter in the Columbia River: In Situ Sensors Elucidate Biogeochemical and Molecular Analyses." *Biogeosciences Discuss* 1–33. doi:10.5194/bg-2016-263.
- Wunsch, U. J., K. R. Murphy, and C. A. Stedmon. 2017. "The One-Sample PARAFAC Approach Reveals Molecular Size Distributions of Fluorescent Components in Dissolved Organic Matter." *Environmental Science & Technology* 51 (20): 11900–11908. doi:10.1021/acs.est.7b03260.
- Wünsch, U. J., K. R. Murphy, and C. A. Stedmon. 2015. "Fluorescence Quantum Yields of Natural Organic Matter and Organic Compounds: Implications for the Fluorescence-Based Interpretation of Organic Matter Composition." *Frontiers in Marine Science* 2. doi:10.3389/fmars.2015.00098.
- Yakimenko, O., D. A. Khundzhua, A. Izosimov, V. Yuzhakov, and S. Patsaeva. 2018. "Source Indicator of Commercial Humic Products: UV-Vis and Fluorescence Proxies." *Journal of Soils and Sediments* 18 (4): 1279–1291. doi:10.1007/s11368-016-1528-9.
- Zepp, R. G., and P. F. Schlotzhauer. 1981. "Comparison of Photochemical Behavior of Various Humic Substances in Water: III. Spectroscopic Properties of Humic Substances." *Chemosphere* 10 (5): 479–486. doi:10.1016/0045-6535(81)90148-X.
- Zepp, R. G., W. M. Sheldon, and M. A. Moran. 2004. "Dissolved Organic Fluorophores in Southeastern US Coastal Waters: Correction Method for Eliminating Rayleigh and Raman Scattering Peaks in Excitation-Emission Matrices." *Marine Chemistry* 89 (1–4): 15–36. doi:10.1016/j.marchem.2004.02.006.
- Zsolnay, A., E. Baigar, M. Jimenez, B. Steinweg, and F. Saccomandi. 1999. "Differentiating with Fluorescence Spectroscopy the Sources of Dissolved Organic Matter in Soils Subjected to Drying." *Chemosphere* 38 (1): 45–50. doi:10.1016/S0045-6535(98)00166-0.